

Dynamic Behavior of Single-Phase Natural Convection Loops

Leon Lima¹

Programa de Pós-graduação em Engenharia Mecânica, UERJ, Rio de Janeiro

Norberto Mangiavacchi²

Faculdade de Engenharia Mecânica, UERJ, Rio de Janeiro

Abstract. Single-phase Natural Convection Loops (NCL's) are engineering solutions to perform the function of heat removal without external energy supply. Nuclear Power Industry is, perhaps, the most important application of NCL's. Greater reliability and lower costs are advantages of such systems in comparison to active ones. The counterpart is the possibility of unstable behavior to show up for certain operating and constructing parameters. The interest of the present work is on the dynamic behavior of the single-phase variance of NCL's. A 1D model has been implemented to perform both linear and non-linear stability analysis. This work shows how operating and geometrical parameters impact on the dynamic behavior of single-phase NCL's.

Keywords. Dynamical System, Stability Analysis, Natural Convection, Passive Safety Systems

1 Introduction

The interest in Natural Convection Loops (NCL's) has increased considerably after the events of Fukushima, in 2011, when three core meltdowns occurred in a Nuclear Power Station of Fukushima Daiichi, after the catastrophic tsunami that hit the east coast of Japan. The outcomes from this accident have pushed new designs of nuclear power plants to incorporate passive safety systems, so that in the scenario of a loss of external energy supply, cooldown of the plant is still possible. Besides, passive systems are cheaper and provide enhanced reliability in comparison to active ones. However, since there are no active control mechanisms, passive systems are more susceptible to unstable behaviors.

NCL's are a type of passive system to perform the function of heat removal. They can operate in single or two-phase flow regime (for subcritical thermodynamic conditions).

This work consists on a numerical study of the dynamic behavior of single-phase NCL's as a function of the operating and geometrical parameters. The platform for the study was a 1D model, based on momentum and energy balances in the loop. A linearized version of perturbed form of equations has also been implemented to perform linear stability analysis.

¹matosleon@gmail.com

²norberto@gmail.com

2 Mathematical Model

The basic structure of the NCL's considered in this work consists of a heater and a cooler connected by pipes, forming a rectangular circuit. Heater and cooler consist of tube sections with conducting walls and can be vertical or horizontal. It reproduces the dimensions of the experimental NCL installed in Bhabha Atomic Research Centre (BARC), in Mumbai, India, described by [1]. Figure 1 shows a schematic drawing of the circuit.

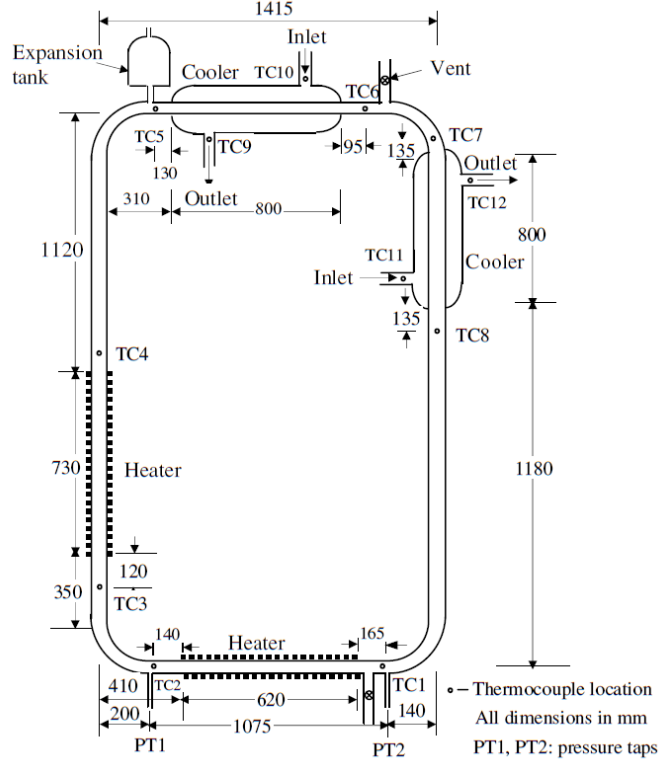


Figure 1: Dimensional drawing of experimental NCL constructed at BARC. The figure is an extraction from [1].

Note that the loop is provided with both vertical and horizontal heaters and coolers, with the objective to observe the influence of the orientation of these components, which is actually the main topic of [1]. They have found that the most unstable configuration is that of horizontal heater and cooler (HHHC configuration).

It is assumed that all properties are constant in the cross section area. The circuit walls are assumed to be adiabatic along the entire loop except for heaters and coolers. Axial heat conduction is neglected, as well as viscous heating. After the a.m. assumptions, the mathematical model consists on the momentum and energy conservation equations given by

$$\frac{L}{A} \frac{dw}{dt} = - \left(f \frac{L}{D} + K \right) \frac{w^2}{2\rho_0 A^2} + \rho_0 g \beta \oint T dz \quad (1)$$

$$\text{heater: } \frac{\partial T}{\partial t} + \frac{w}{\rho_0 A} \frac{\partial T}{\partial s} = \frac{Q}{L_h A \rho_0 c_p} \quad (2a)$$

$$\text{cooler: } \frac{\partial T}{\partial t} + \frac{w}{\rho_0 A} \frac{\partial T}{\partial s} = -\frac{4U(T - T_s)}{D \rho_0 c_p} \quad (2b)$$

$$\text{pipes: } \frac{\partial T}{\partial t} + \frac{w}{\rho_0 A} \frac{\partial T}{\partial s} = 0 \quad (2c)$$

In equation 1: L , D and A are the length, diameter and cross section area (constant) of the loop, respectively, and $w = \frac{1}{\rho A} \int_0^L u dA$ is the system's mass flow rate, t is time, f is friction factor, K is the local losses coefficient, ρ is the fluid density, g is the module of gravity field. Boussinesq hypothesis is adopted to write density as a linear function of temperature in the gravity term of momentum equation to solve the inconsistency between incompressibility assumption and the presence of buoyancy. Thus, density is written as $\rho = \rho_0[1 - \beta(T - T_0)]$, where the subscript 0 represents a value based on mean temperature value and β is the thermal expansion coefficient (also evaluated at T_0). The friction factor f and K were introduced.

In equation 2: T is the temperature field, s is the space coordinate in axial direction, Q is the total heat input rate, L_h is the heater length, c_p is the specific heat at constant pressure, U is the heat transfer coefficient in the cooler, T_s is the temperature of the cold source.

The friction factor f can be calculated by many correlations. For natural convection in tubes, it is still common practice to employ forced flow correlations, like Poiseuille's ($f = 64/\text{Re}$, in laminar regime), Blasius' ($f = 0.316/\text{Re}^{0.25}$, in turbulent regime) and others. In this work, a combination of Poiseuille's correlation with that of Colebrook is employed. There are many works which tried to establish a suitable correlation for natural convection, but none has covered a wide range of flow regimes or loop configuration. Even in the case of the classical correlations for forced flow, considerable differences may appear. [2] have addressed this topic, arguing that single-phase NCL typically operate in the transitional range, where friction correlations differ most.

3 Linear Stability Model

To evaluate the stability of a NCL by the balance equations, i.e., by transient calculations, can be a costly option if a wide range of parameters has to be considered. So linear stability analysis can be a valuable tool in such situations. It provides a measure of the system's response to small perturbations, assuming that non-linear effects can be neglected. This hypothesis do not apply for large perturbations. In this work, linear analysis is used to generate a stability map for the NCL described in the previous section, as a function of heat transfer coefficient U and the heat input Q . The following section will make use of this map to analyze non-linear response for three selected operating points in the map.

Stability analysis is performed by the solution of an eigenvalue problem, obtained by the perturbed version of equations 1 and 2. Introducing the decomposition given by

$$w = \bar{w} + \hat{w}e^{\lambda t} \quad (3a)$$

$$T = \bar{T} + \hat{T}(s)e^{\lambda t} \quad (3b)$$

into equations 1 and 2, with $\lambda \in \mathbb{C}$, we arrive at the system of equations given by 4 and 5.

$$\lambda \hat{w} = - \left(f \frac{L}{D} + K \right) \frac{\bar{w} \hat{w}}{\rho_0 L A} - \hat{w} f' \frac{\bar{w}^2}{2D \rho_0 A} + \frac{A}{L} \rho_0 g \beta \oint \hat{T} dz \quad (4)$$

$$\lambda \hat{T} + \frac{\bar{w}}{\rho_0 A} \hat{T}' + \frac{\hat{w}}{\rho_0 A} \bar{T}' = - \frac{4U \hat{T}}{D \rho_0 c_p} \quad (5a)$$

$$\lambda \hat{T} + \frac{\bar{w}}{\rho_0 A} \hat{T}' + \frac{\hat{w}}{\rho_0 A} \bar{T}' = 0 \quad (5b)$$

In equations 3, \bar{w} and \bar{T} define the steady state condition and \hat{w} and \hat{T} are the amplitude of the perturbations, where \hat{w} is constant and $\hat{T} = \hat{T}(s)$ is a function of s .

4 Stability map

The linear stability model has been employed to generate a stability map for a range of heat transfer coefficient U (of the cooler) and the heat input Q . The choice for these two parameters follows the stability maps generated by [3]. In that work the authors performed linear stability analysis for the four loop configurations, for the domain defined by $300 < U < 1000$ W/m²/K and $100 < Q < 800$ W, and observed instability only for the HHHC configuration. For this reason, fig. 2 shows the stability map only the HHHC. Table 1 summarizes the geometrical and operating parameters of the loop.

internal diameter [mm]	26.9
loop height [m]	2.200
loop width [m]	1.415
heater length [m]	0.620
cooler length [m]	0.800
local losses	4.2
mesh nodes	1200
Q [kW]	0.1 – 0.8
U [kW/m ² /°C]	0.3 – 1.0
friction correlation	Poiseuille-Colebrook
T_s [°C]	30

Tabela 1: Geometric, operating and numerical data for the HHHC 26.9 mm diameter loop.

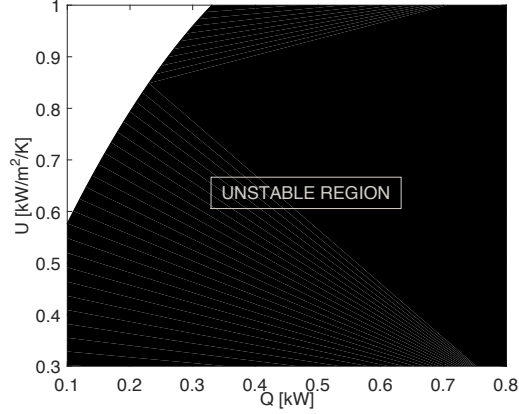


Figura 2: Stability map for HHC configuration of 26.9 mm diameter loop from [1].

Immediate conclusion is that increasing Q produces “increasing instability”, while increasing U tends to stabilize the system. The transient results that will be shown in the next section are based on this map, where stable behaviors are expected from the white area, and increasing oscillations are expected for the other regions.

5 Transient Results

Transient calculations were performed for the parameters listed in table 1, using $CFL = 1$. CFL is a parameter for numerical stability defined as $CFL = u\Delta t/\Delta s$. In this code, CFL is an input for the calculation of Δt , which is given by $\Delta t = \min(\frac{CFL\Delta s}{u}, \Delta t_{\max})$, where Δt was set at 0.1. This aspect of numerical formulation is discussed in [4]. In the following, the transient result for three points in the map of fig. 2 are presented, all for $U = 0.8 \text{ kW/m}^2/\text{K}$: $Q = 0.1 \text{ kW}$, $Q = 0.2 \text{ kW}$ and $Q = 0.4 \text{ kW}$. The object was to have a sample of a stable system, a neutral system and an unstable system. For the unstable case ($Q = 0.4 \text{ kW}$), a second simulation was performed which considered $CFL = 0.1$. For each case, the frequency domain is presented. In all simulations, the initial mass flow was set to zero.

Figure 3 shows a stable case and a slightly unstable case, both dominated by a single oscillating mode. Larger amplitudes are observed for the case of $Q = 0.2 \text{ kW}$. It is interesting to note that for point $Q = 0.2 \text{ kW}$ and $U = 0.8 \text{ kW/m}^2/\text{K}$, although located in the stable region of the stability map, the system presents increasing oscillations, which may denote the results of non-linear effects.

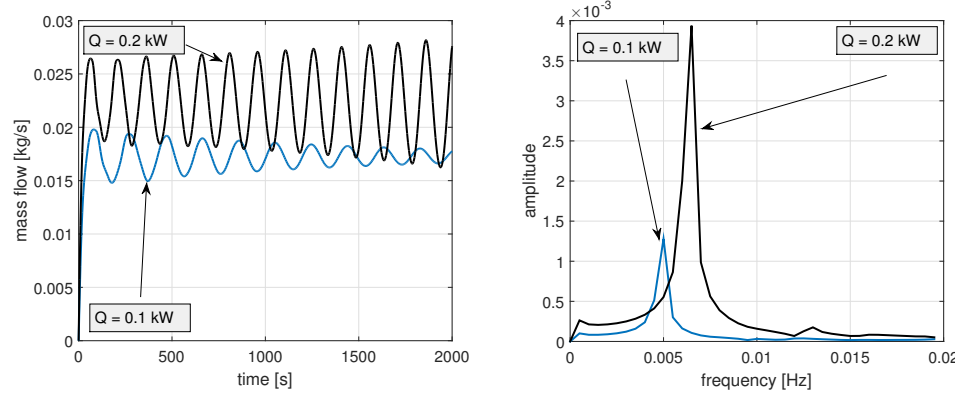


Figure 3: Comparison of transient results and frequency spectra of NCL with $U = 0.8$ $\text{kW/m}^2/\text{K}$ for two heat input values: $Q = 0.1$ kW and $Q = 0.2$ kW.

Figure 4 presents the transient for the unstable operating point $Q = 0.4$ kW and $U = 0.8$ $\text{kW/m}^2/\text{K}$. Oscillations grow up to flow reversal, when the system seems to reach a limit cycle. Fourier transform shows two predominant modes in the range between the two red dots.

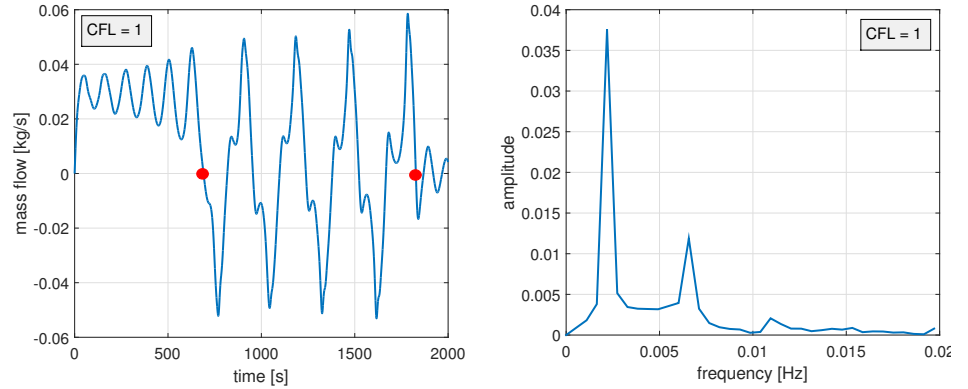


Figure 4: Transient and frequency spectrum of NCL with $Q = 0.4$ kW and $U = 0.8$ $\text{kW/m}^2/\text{K}$.

The same point, but with CFL reduced to 0.1, produces quite different behavior. A non-symmetrical oscillating regime takes place after flow reversal. The frequency spectrum (performed over the range between the red dots) shows several oscillating modes, one of them with predominantly larger amplitude.

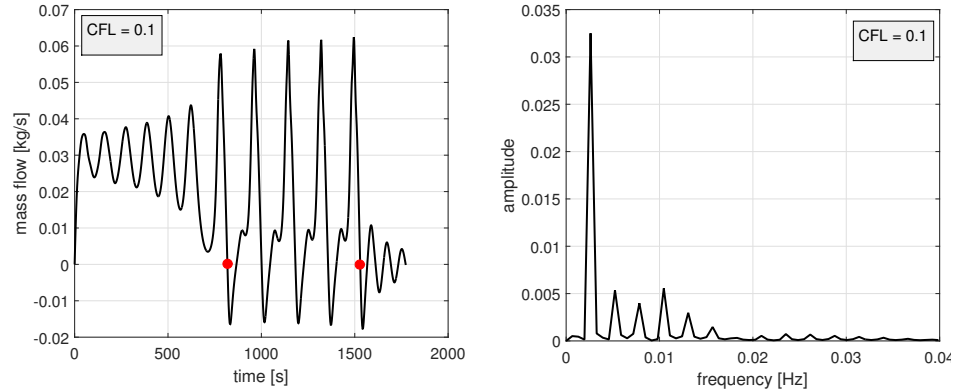


Figure 5: Transient and frequency spectrum of NCL with $Q = 0.4$ kW and $U = 0.8$ kW/m²/K, with CFL reduced from 1 to 0.1.

6 Conclusions

Firstly, it can be concluded that the results from non-linear calculation agreed well with the linear stability model.

For the HHHC configuration studied, stable systems show oscillating behavior dominated by a single mode after a perturbation, and unstable systems present growing amplitude of oscillations, also in a single frequency, until flow reversal occurs. After reversal, depending on geometrical and operating parameters, other modes may appear in the system's dynamics.

It was also observed that the numerical formulation influences the results, like modifying the CFL number.

Referências

- [1] P.K. Vijayan, M. Sharma, and D. Saha. Steady state and stability characteristics of single-phase natural circulation in a rectangular loop with different heater and cooler orientations. *Experimental Thermal and Fluid Sciences*, 31:925–945, 2007.
- [2] W. Ambrosini, N. Forgione, J. C. Ferreri, and M. Bucci. The effect of wall friction in single-phase natural circulation stability at the transition between laminar and turbulent flow. *Annals of Nuclear Energy*, 31:1833–1865, 2004.
- [3] D. S. Pilkhwal, W. Ambrosini, N. Forgione, P. K. Vijayan, D. Saha, and J. C. Ferreri. Analysis of the unstable behaviour of a single-phase natural circulation loop with one-dimensional and computational fluid-dynamic models. *Annals of Nuclear Energy*, 34:339–355, 2007.
- [4] Leon Lima and Norberto Mangiavacchi. 1D stability analysis of single-phase Natural Circulation Loops. In *Inproceedings of COBEM 2015, Rio de Janeiro*, 2015.